Original
Nuclear Medicine Review 2019, 22, 2: 60–68
DOI: 10.5603/NMR.a2019.0014
Copyright © 2019 Via Medica
ISSN 1506–9680

VIA MEDICA

Three-compartment pharmacokinetic models of radiotracers used in the GFR-determination — estimation of their parameters using the time-concentration curves

Cyprian Świętaszczyk[1], Lars Jødal[2]

[1]Department of Nuclear Medicine, Citomed, Toruń, Poland
[2]Department of Nuclear Medicine, Aalborg University Hospital, Denmark

[Received 18 XII 2019; Accepted 4 VI 2019]

ABSTRACT

BACKGROUND: In GFR measurements with radiotracers, there is evidence that a two-compartment model is unable to describe the full plasma curve, including early time points, but analyses generally focus on two-compartment models.
AIMS: To analyze both the mammillary and catenary three-compartment model and to determine empirical relations between model constants and the overall GFR and ECV (extra-cellular volume).
MATERIAL AND METHODS: Mathematical analysis of the three-compartment model. Full-curve patient data from 32 adults and 7 children were used to relate model parameters to GFR and ECV.
RESULTS: Model volumes were found to be roughly proportional to ECV. In both models, the central (plasma) volume was $V_1 = 0.24 \times ECV$ and elimination rate from V_1 was $k_{10} = 4.2 \times GFR/ECV$. In the mammillary model, the two parallel volumes were $V_2 = 0.28 \times ECV$, $V_3 = 0.48 \times ECV$, and intercompartmental clearances were Cl_{12} [mL/min] $= 0.0058 \times ECV$ [mL], $Cl_{13} = 0.042 \times ECV$. In the catenary model, the serial volumes were $V_2 = 0.60 \times ECV$, $V_3 = 0.16 \times ECV$, with clearances $Cl_{12} = 0.048 \times ECV$, $Cl_{23} = 0.0036 \times ECV$.
CONCLUSION: Insight into the three-compartment model was achieved, and empirical relations to ECV and GFR/ECV were determined.

KEY words: GFR-determination, pharmacokinetics, compartment model, Tc-99m-DTPA

Nucl Med Rev 2019; 22, 2: 60–68

Introduction

Although inulin-clearance is still regarded as the gold standard in the glomerular filtration rate (GFR) assessment, radionuclide methods with application of chromium-51-ethylene-diamine-tetraacetate (Cr-51-EDTA) and technetium-99m-diethylele-triamine-pentaacetate (Tc-99m-DTPA) have the dominant position [1]. It is widely accepted that both radiotracers are characterized by a very similar behavior after injection to human plasma [2–5]. However, none of these papers developed a pharmacokinetic model of these tracers, i.e., it is still impossible to forecast the behavior of these tracers (concentrations, time-concentration curve parameters) in the plasma after injection. Fleming [6] analyzed a two-compartment model. However, description of the full plasma curve (including the fast early behavior) requires at least three exponential functions [7], which for a compartment model corresponds to at least three compartments.

The aim of this study is to explore three-compartment models with central elimination and determine how the detailed parameters of the model relate to the GFR and extracellular volume (ECV). More specifically, based on the model and patient data, the study will attempt to predict the patient-specific micro-parameters of the compartment model, given the GFR and ECV of the patient, and thus to predict the behavior of the tracers in the plasma after the injection.

Correspondence to: Cyprian Świętaszczyk,
Zakład Medycyny Nuklearnej, Lecznice Citomed,
ul. Marii Skłodowskiej-Curie 73, 87–100 Toruń;
e-mail: c.swietaszczyk@bieganski.org

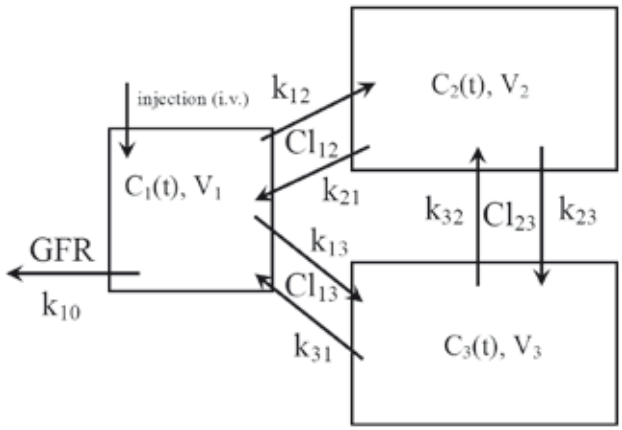

Figure 1. The pharmacokinetic models with central elimination considered in this study (see the text for the explanations). In the mammillary model, $Cl_{23} = k_{23} = k_{32} = 0$; in the catenary model, $Cl_{13} = k_{13} = k_{31} = 0$

Theory of the compartment model and GFR determination

The models considered in this study are shown in Figure 1. They consist of the central compartment (*1*; i.e., the plasma) and two tissue-fluid compartments (*2* and *3*). C_i and V_i are the concentration and the volume, respectively, of the compartment showed by the lower index. The sum of the volumes of all three compartments makes together the extracellular volume (*ECV*).

It is assumed that the radiotracer intercompartmental transport is passive with a rate that is proportional to the concentration. According to the widely accepted convention, the respective transport rate constants (*k*) have lower indices denoting the direction of the transport, e.g., k_{12} is the elimination rate constant from compartment *1* to *2*, k_{21} from *2* to *1*. The k_{10} is the elimination rate constant from the compartment *1* to the environment, i.e., extraction of the tracer by the kidneys resulting in excretion from the blood to the bladder.

Since the intercompartmental transport is passive, the following exemplary relationship is fulfilled:

$$Cl_{12} = k_{12} \times V_1 = k_{21} \times V_2 \quad \{1\}$$

where Cl_{12} is the intercompartmental clearance (the same in both directions). Additionally:

$$GFR = k_{10} \times V_1 \quad \{2\}$$

In this work, volumes are expressed in milliliters [mL], time in minutes [min], clearances in mL/min, and elimination rate constants in min^{-1}.

The terms k_{ij}, V_i and Cl_{ij} are called the system micro-constants. The plasma concentration in any time point *t* following the bolus i.v.-injection can be expressed with a three-exponential formula:

$$C_1(t) = \sum_{i=1}^{3} c_i \times \exp(-b_i \times t) \quad \{3\}$$

where the convention here will be that $i=1$ denotes the slowest, $i=2$ the middle, and $i=3$ the fastest component, i.e. $b_1 < b_2 < b_3$. The above parameters b_i and c_i are called the system macro- or hybrid constants (or the curve parameters). The algorithm transforming the micro-constants into the hybrid-constants is given in the Appendix 1.

The GFR (more precisely: the radiotracer clearance) can be calculated as:

$$GFR = \frac{Q}{AUC} \quad \{4\}$$

where *Q* is the injected amount (activity) of the tracer, and *AUC* is the area under the plasma time-concentration curve (decay-corrected). *AUC* in turn can be obtained as:

$$AUC = \sum_{i=1}^{n} c_i / b_i \quad \{5\}$$

where $n=3$ in the case of three-exponential curve.

Likewise, the total extracellular volume (ECV) can be calculated as [8]:

$$ECV_{fc} = Q \frac{\sum_{i=1}^{n} \frac{c_i}{b_i^2}}{AUC^2} \quad \{6\}$$

A set of time-concentration points can be transformed into the time-concentration curve by use of an algorithm referred to as "curve-stripping" or "curve peeling-off" [7, 9]. Because, in clinical circumstances, this procedure (engaging multiple plasma sampling) is cumbersome, methods for estimation of the GFR from the final slope of the curve have been developed, e.g. [7, 10, 11]. This allowed reducing the number of necessary plasma samples to just a few (even two) a few hours following the radiotracer injection.

As mentioned in the introduction, a two-compartment model (2-C) cannot fully describe the plasma concentration curve [7]. The physiological reality may be even more complex than a three-compartment model, but the concentrations in the early phase change very fast and their precise determination is difficult, so an extraction of a four- or more-exponential curve from the time-concentration data is problematic. This limits the number of parameters that can robustly be modeled. A mathematical analysis of a four-compartment (4-C) model would also be far more complicated [12–14].

Physiologically, GFR is primarily a result of the effectiveness of the kidneys. Except for k_{10}, the k_{ij} parameters express the ability of tracer to move between body compartments not directly related to the kidneys. Our model will assume these k_{ij} parameters to be person-independent. Except for cases of edema, the compartment volumes V_i will also be only little affected by renal function. Our model will assume V_i's to scale with *ECV*, but otherwise be person-independent. Together, these two assumptions result in the expectation of Cl_{ij} also scaling with *ECV* (cf. equation {1}).

Both a mammillary and a catenary model will be investigated. The universal 3-compartment model (see Fig. 1) would involve more *k* parameters and is not considered in this study.

Materials and methods

Patient inclusion criteria

The patient data were got from the database of Prof. Brøchner-Mortensen used in previous works [7, 10, 11]. Inclusion criterion for the present study were measured plasma volume (and hence initial concentration), as well as concentration values measured

in all of the time points 15, 30, 60, 90, 120, 150, 180, 210, 240, 270 and 300 minutes. For the timing, up to 10% deviation from the time point was allowed (e.g. 30 ± 3 minutes was acceptable). This resulted in inclusion of 32 adults and 7 children. The patient group consisted of subjects with normal as well as with impaired renal function. For 4 adults and all 7 children, early time-points at 5 and 10 minutes were also accessible.

Reconstruction of the time-concentration curve

In the following, the original time-concentration points are referred to as "genuine points". The time-concentration curve was reconstructed according to the procedure described originally by Brøchner-Mortensen [7]. Shortly, the parameters of the slowest component (slope, *b1*, and intercept, *c1*) were obtained by linear regression of the logarithmized 5 last time-concentration points (180 to 300 minutes). The reconstruction of the middle and the fastest component followed by the "curve-stripping" method; the numbers of the time-concentration points processed in each of these steps ranged from two to five. Thus, the complete three-exponential time-concentration curve was reconstructed (b_1, b_2, b_3, c_1, c_2, c_3).

Establishing of input ECV, GFR and micro-constants for each patient

For the processing, only full-curve data were used. Full-curve results GFR_{fc} and ECV_{fc} were calculated with equations {4} to {6}.

Then, the micro-constants of the mammillary model were determined for each patient separately using the algorithm given in the Appendix 2.

Averaging and regression of the individual data

For each subject, the obtained micro-constants were divided by the *ECV*, and these data were averaged and regressed to obtain formulas for calculation of compartment volumes and intercompartmental clearances as functions of *ECV*. We tested for normality and re-calculated from log-normal distribution for Cl_{12} and Cl_{13}. However, the procedure did not result in overall better fit (results not shown). Accordingly, calculations in the following are based on simple mean values and standard deviations (SD). These procedures were performed for all 39 patients together, as well as separately for adults and children. Then, possible dependences of V_1/ECV, V_2/ECV, V_3/ECV, Cl_{12}/ECV, Cl_{13}/ECV on *ECV* and the subjects' ages and gender were examined in order to verify, whether there is a relationship between these values, and to find the optimal set of input data needed for establishing of the model.

Thus, a general three-compartment mammillary pharmacokinetic model was created. As shown below, the *ECV* and *GFR* were proven to be necessary and sufficient input values for transforming of this general model into the theoretical patient-specific one.

The general mammillary model served to create pattern time-concentration curves. They, in turn, were then transformed into the micro-constants of the three-compartment catenary model according to the algorithm presented in the Appendix 3. We checked numerically that, for each general mammillary model, a general catenary model exists, which is equivalent in respect to the central compartment (i.e., the same *ECV*, V_1, *GFR* and time-concentration curve in the V_1).

Evaluation of the averaged mammillary model

Evaluation from full-curve data

The averaged mammillary model was evaluated using ECV_{fc} and GFR_{fc} as input. For a given patient, the model estimated curve parameters (b_1, b_2, b_3, c_1, c_2, c_3), and thereby also the plasma curves described by these parameters.

Model curve parameters and plasma curve points were compared with the "genuine" results from the full data. Comparison was done by calculation of the relative differences, calculated using the following formula:

$$RD = (G - M)/M \quad \{7\}$$

where:

RD: relative difference,

G: genuine parameter,

M: modeled parameter.

It can be noted that *RD* express the deviation of the genuine data from the modeled data (*M* in the denominator), rather than the other way around. This is to avoid division by a noisy data point. The genuine data contain random noise, while the modeled data may contain bias but are averaged regarding noise. A positive *RD* corresponds to the genuine data point being higher than the model prediction.

Evaluation from slope-intercept data

Having full-curve data available is not the normal situation. So we extended the evaluation to use only the late (3–5 hours p.i.) data, i.e. the data used when GFR is calculated with the slope-intercept method.

In this case, *GFR* and *ECV* were calculated with the formulas of Jødal&Brøchner-Mortensen [8, 10, 11]:

$$GFR_{JBM} = \frac{GFR\beta}{1 + f \times GFR\beta}, \quad \{8\}$$

$$ECV_{JBM} = \frac{V_{da}}{1 + 2 \times f \times GFR\beta}, \quad \{9\}$$

where

$$f = 0.0032 \times BSA^{-1,3} \quad \{10\}$$

BSA is the body surface area [m^2], while V_{da} and $GFR\beta$ are the apparent volume of distribution and the *GFR*-value, respectively, obtained from the final slope of the time-concentration curve:

$$GFR\beta = \frac{Q}{c_1 / b_1} \quad \{11\}$$

$$V_{da} = \frac{Q}{c_1} \quad \{12\}$$

Given GFR_{JBM} and ECV_{JBM} (instead of GFR_{fc} and ECV_{fc}) as input, evaluation proceeded as described above.

Results

General 3-C mammillary pharmacokinetic model

The averaging and regression of the all patients' data delivered the ratios (average ± standard deviation, SD) presented in Table 1.

Table 1. Ratios of the computed model parameters to the ECV (mammillary model)

Ratio	Mean ± SD
V_1/ECV	0.240 ± 0.027
V_2/ECV	0.283 ± 0.101
V_3/ECV	0.477 ± 0.091
Cl_{12}/ECV	0.00578 ± 0.00339
Cl_{13}/ECV	0.0422 ± 0.0160

The largest correlation within the data was found between V_1/ECV and ECV, but it was only $r = -0.35$; the absolute correlation coefficients between the rest of the examined parameters were lower than 0.2. Hence, these relationships were not taken into consideration in the data processing.

Thus, the following formulas were established for the respective micro-constants in the general mammillary model, i.e. the plasma volume V_1 in exchange with both V_2 and V_3 (but no exchange between V_2 and V_3):

$V_1 = 0.24 \times ECV$,

$V_2 = 0.28 \times ECV$,

$V_3 = 0.48 \times ECV$,

$Cl_{12} = 0.0058 \times ECV$ (hence: $k_{12} = 0.0242$, $k_{21} = 0.0207$),

$Cl_{13} = 0.042 \times ECV$ (hence: $k_{13} = 0.175$, $k_{31} = 0.0876$).

$V_1 = 0.24 \times ECV$,

Regarding k_{10} (cf. equation {2}):

$k_{10} = GFR / V_1 = 4.2 \times GFR / ECV$

General 3-C catenary pharmacokinetic model

In the catenary model, plasma volume V_1 is in exchange with the middle volume V_2 which is further in exchange with V_3 (but there is no exchange between V_1 and V_3). Relations were:

$V_1 = 0.24 \times ECV$ (as in the mammillary model),

$V_2 = 0.60 \times ECV$,

$V_3 = 0.16 \times ECV$,

$Cl_{12} = 0.048 \times ECV$ (hence: $k_{12} = 0.199$, $k_{21} = 0.0794$),

$Cl_{23} = 0.0036 \times ECV$ (hence: $k_{23} = 0.00599$, $k_{32} = 0.0228$).

As in the mammillary model:

$k_{10} = GFR / V_1 = 4.2 \times GFR / ECV$

Comparison of the reconstructed curve parameters and genuine concentrations to the values predicted by the mammillary model

For both adults and children, the relative differences (RD in eq. {7}) of the macroparameters (Tab. 2) and concentrations (Fig. 2–5) were calculated twice. First using full-curve data for ECV and GFR as model input (fc-data), second using ECV and GFR calculated with the respective JBM-formula as model input (JBM-data).

Table 2: Relative differences (cf. eq. {7}) for macroparameters calculated either from genuine, individual patient data, or from the mammillary model predictions, using GFR and ECV as input. Differences are presented as mean (SD), separately for adults (n = 32) and children (n = 7)

Parameter	Adults, fc-data *	Children, fc-data *	Adults, JBM-data†	Children, JBM-data†
b_1	–1.4 (3.9) %	0.71 (7.5) %	1.1 (1.9) %	2.8 (4.0) %
c_1	–2.9 (8.9) %	1.5 (19) %	2.4 (4.6) %	6.4 (9.8) %
b_2	–6.4 (34) %	20 (51) %	–6.2 (34) %	21 (50) %
c_2	3.0 (49) %	34 (54) %	12 (55) %	52 (70) %
b_3	–5.4 (34) %	34 (21) %	–5.2 (34) %	35 (21) %
c_3	2.6 (16) %	–3.9 (10) %	10 (22) %	4.2 (18) %

*Full-curve data were used to calculate GFR and ECV for model input
† Only late data points and the JBM corrections were used to calculate GFR and ECV for model input (slope-intercept method, cf. eqs. {8} and {9})

Discussion

The resulting general models give theoretical compartment volumes and intercompartmental clearances which are simple fractions of the entire extracellular volume. It corresponds to assuming that the intercompartmental exchange rates are independent from the ECV. A slight negative correlation between V_1/ECV and ECV was found, but this correlation was considered weak. Indeed, a further pursuing of the weak relationship made all the resulting formulas for the respective compartment volumes and intercompartmental clearances (or elimination rate constants) more complicated, but the ultimate precision of the model remained virtually the same (data not presented).

To our knowledge, this is the first study elucidating three-compartment pharmacokinetic models of these radiotracers, so that any prediction of the behavior of the tracer after its injection to a patient with known GFR and ECV is possible. Fleming presented a model with a single extra-vascular compartment [6], but such a compartment will correspond to a two-exponential plasma concentration. A two-exponential function can describe most of the plasma concentration curve, but cannot include the quick fall in the earliest part of the curve.

Our model predicted the curve parameters and the concentrations with similar accuracy when the full-curve GFR and ECV as well as the JBM-data served as the input. It leads to the conclusion that the model can be useful with the data just approached by the formulas from the late time-concentration points. It seems to additionally support that the JBM formulas offer very reliable results in comparison to the full-curve data which in turn can be got only with a logistically cumbersome procedure of multiple blood withdrawals during a long time period in each patient. The application of the JBM formulas allows reducing the number of blood samplings to a few, sometimes even two, performed solely 3–5 hours following the injection.

The predictions on the curve parameters and the concentrations were generally less accurate in pediatric patients; especially the SD-values were higher: it seemed to hint at a higher

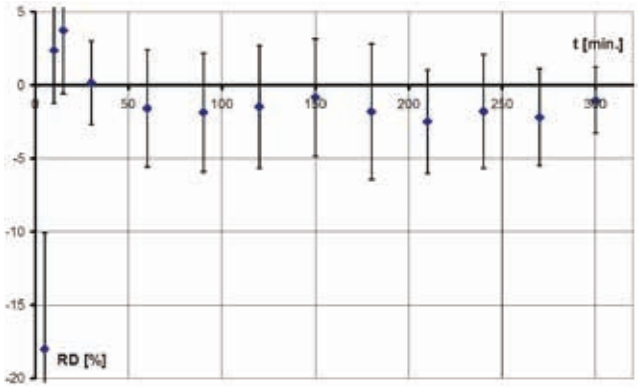

Figure 2. Relative differences (RD ± SD) between genuine and model concentrations in the respective time points for adults, using full-curve values ECV_{fc} and GFR_{fc} as model input. For the time points 5 and 10 minutes, $n = 4$, for the rest of the parameters, $n = 32$

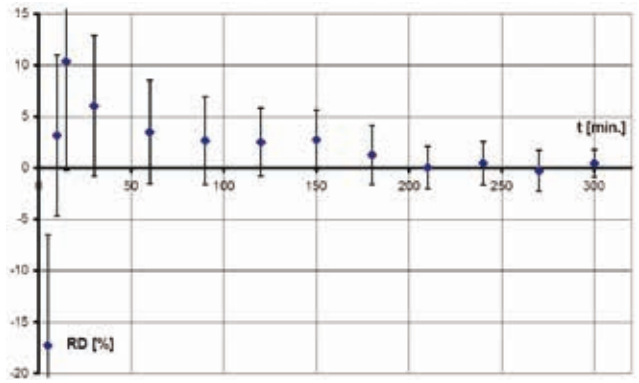

Figure 4. Relative differences (RD ± SD) between genuine and model concentrations in the respective time points for adults, using final-slope values ECV_{JBM} and GFR_{JBM} as model input. For the time points 5 and 10 minutes, $n = 4$, for the rest of the parameters, $n = 32$

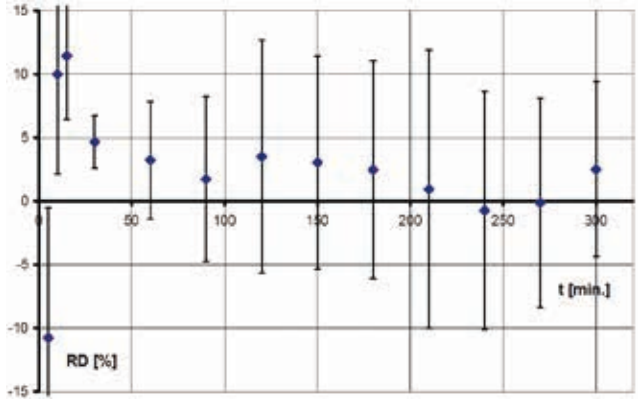

Figure 3. Relative differences (RD ± SD) between genuine and model concentrations in the respective time points for children, using full-curve values ECV_{fc} and GFR_{fc} as model input; $n = 7$

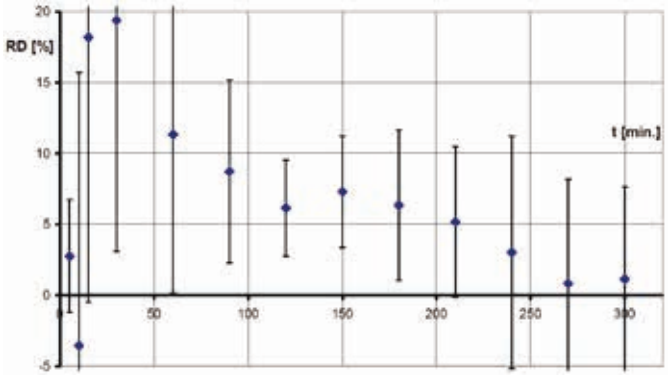

Figure 5. Relative differences (RD ± SD) between genuine and model concentrations in the respective time points for children, using final-slope values ECV_{JBM} and GFR_{JBM} as model input; $n = 7$

interpersonal variability in the pediatric group rather than at a different set of averaged micro-parameters that should be used for pharmacokinetic studies.

At the late time points, almost all genuine concentrations deviate from the modeled ones by no more than a few percent. It can be noticed from Figures 2–5, though, that deviations are somewhat systematic for the first hour or two, and largest for the earliest time points. A similar tendency can be observed for the curve parameters (Tab. 2). These factors hint at a higher interpersonal variability of the early phase as compared to the later phases. The following reasons seem to be potentially responsible for this phenomenon:

First, the developed three-compartment mammillary model is only an approximation of the real biologic situation which in turn hypothetically could be described by a very complex multicompartment model. Still, the three-compartment model can be expressed as a unique analytical solution, as demonstrated here and elsewhere [12, 15, 16]. A four-compartment model, although potentially more punctual, is characterized by a much higher complexity [13, 14]. For higher models, such analytic solutions have not been found, although numerical models exist. Moreover, whereas it is possible to create pharmacokinetic models with different numbers of compartments and parallel with the same late phase of the time-concentration curve, the early phases must show significant differences in such a comparison.

Second, several factors contribute to the precision of the concentration measurement. Beyond the accuracy of the timing, sampling (volume) and counting, the place of the blood withdrawal seems to have a significance: The mathematical models assume a uniform distribution of the concentration within the entire blood, whereas it seems obvious that the concentration in the upper proximity vein (the most popular location of blood sampling) can differ from the concentration in, for example, renal vein or renal artery. These differences are the most pronounced in the early phase, where a rapid decrease of the serum concentration is observed.

Moreover, all the calculations are performed with the next assumption of instantaneous mixing of the injected radiotracer with the entire blood; this is the next condition that is actually not fulfilled. Hence, the practically measured early phase concentrations are more likely to differ from the model than the later phase.

Summing up, a development of a theoretically more precise higher compartment model would constitute a mathematical challenge, and, practically, it would potentially give only little added value to the pharmacokinetics of the radiotracers applied in the

assessment of the glomerular filtration rate, with practically no possibility of its verification.

Conclusions

A model has been set up, which can be analytically studied. The model was to a reasonable extent able to reproduce the patient curves. The model is patient-specific in the sense that given GFR and ECV, it can be used to estimate the microconstants, and further the time-concentration curve parameters and the concentrations, for this patient.

Acknowledgments

Prof. Jens Brøchner-Mortensen is thankfully acknowledged for sharing the patient data used in the study.

Sources of support of the work:

none

Conflict of interests:

none perceived

References

1. Murray AW, Barnfield MC, Waller ML, et al. Assessment of glomerular filtration rate measurement with plasma sampling: a technical review. J Nucl Med Technol. 2013; 41(2): 67–75, doi: 10.2967/jnmt.113.121004, indexed in Pubmed: 23658207.
2. Rehling M, Møller ML, Thamdrup B, et al. Simultaneous measurement of renal clearance and plasma clearance of 99mTc-labelled diethylenetriaminepenta-acetate, 51Cr-labelled ethylenediaminetetra-acetate and inulin in man. Clin Sci (Lond). 1984; 66(5): 613–619, indexed in Pubmed: 6423339.
3. Fleming JS, Wilkinson J, Oliver RM, et al. Comparison of radionuclide estimation of glomerular filtration rate using technetium 99m diethylenetriaminepentaacetic acid and chromium 51 ethylenediaminetetraacetic acid. European Journal of Nuclear Medicine. 1991; 18(6): 391–395, doi: 10.1007/bf02258429.
4. Biggi A, Viglietti A, Farinelli MC, et al. Estimation of glomerular filtration rate using chromium-51 ethylene diamine tetra-acetic acid and technetium-99m diethylene triamine penta-acetic acid. Eur J Nucl Med. 1995; 22(6): 532–536, indexed in Pubmed: 7556298.
5. Fleming JS, Zivanovic MA, Blake GM, et al. British Nuclear Medicine Society. Guidelines for the measurement of glomerular filtration rate using plasma sampling. Nucl Med Commun. 2004; 25(8): 759–769, indexed in Pubmed: 15266169.
6. Fleming JS. An improved equation for correcting slope-intercept measurements of glomerular filtration rate for the single exponential approximation. Nucl Med Commun. 2007; 28(4): 315–320, doi: 10.1097/MNM.0b013e328014a14a, indexed in Pubmed: 17325596.
7. Bröchner-Mortensen J. A simple method for the determination of glomerular filtration rate. Scand J Clin Lab Invest. 1972; 30(3): 271–274, indexed in Pubmed: 4629674.
8. Jødal L, Brøchner-Mortensen J. Simplified methods for assessment of renal function as the ratio of glomerular filtration rate to extracellular fluid volume. Nucl Med Commun. 2012; 33(12): 1243–1253, doi: 10.1097/MNM.0b013e3283591908, indexed in Pubmed: 23111354.
9. Dunne A. An iterative curve stripping technique for pharmacokinetic parameter estimation. J Pharm Pharmacol. 1986; 38(2): 97–101, indexed in Pubmed: 2870170.
10. Jødal L, Brøchner-Mortensen J. Reassessment of a classical single injection 51Cr-EDTA clearance method for determination of renal function in children and adults. Part I: Analytically correct relationship between total and one-pool clearance. Scand J Clin Lab Invest. 2009; 69(3): 305–313, doi: 10.1080/00365510802566882, indexed in Pubmed: 19048437.
11. Brøchner-Mortensen J, Jødal L. Reassessment of a classical single injection 51Cr-EDTA clearance method for determination of renal function in children and adults. Part II: Empirically determined relationships between total and one-pool clearance. Scand J Clin Lab Invest. 2009; 69(3): 314–322, doi: 10.1080/00365510802653680, indexed in Pubmed: 19191067.
12. Plusquellec Y. Analytical study of three-compartment pharmacokinetic models: concentration, area under curves, mean residence time. J Biomed Eng. 1989; 11(4): 345–351, indexed in Pubmed: 2619796.
13. Plusquellec Y, Houin G. Analytical study of open four compartment pharmacokinetic models: concentrations, area under curves, mean residence times. J Biomed Eng. 1990; 12(4): 358–364, indexed in Pubmed: 2395363.
14. Biasi Jde. Four open mammillary and catenary compartment models for pharmacokinetics studies. Journal of Biomedical Engineering. 1989; 11(6): 467–470, doi: 10.1016/0141-5425(89)90041-1.
15. Upton RN. Calculating the hybrid (macro) rate constants of a three-compartment mamillary pharmacokinetic model from known micro-rate constants. J Pharmacol Toxicol Methods. 2004; 49(1): 65–68, doi: 10.1016/j.vascn.2003.09.001, indexed in Pubmed: 14670695.
16. Dubois A, Bertrand J, Mentré F. Mathematical expressions of the pharmacokinetic and pharmacodynamic models implemented in the PFIM software. INSERM, University Paris Diderot 2011 (UMR738); accessible: http://www.pfim.biostat.fr/PFIM_PKPD_library.pdf.
17. Fisher D, Shafer S. Fisher/Shafer NONMEM Workshop Pharmacokinetic and Pharmacodynamic Analysis with NONMEM. Het Pand, Ghent, Belgium 2007. https://wiki.ucl.ac.uk/download/attachments/23206987/Shafer%20NONMEM.pdf.
18. Rescigno A. Foundations of pharmacokinetics. Kluwer Academic Publishers. 2004.

Appendix 1. Calculation of the hybrid--constants from the micro-constants of the 3-C mammillary model

The formulas for the central compartment cited from [16], a similar algorithm is given in [17].

The concentration in the central compartment (plasma):

$$C_{1t} = c_1 \times \exp(-t \times b_1) + c_2 \times \exp(-t \times b_2) + c_3 \times \exp(-t \times b_3), \quad \{A1.1\}$$

where index 1: the slowest component, 3: the fastest component;

If the differential equations describing the concentrations in the compartments are transformed into the matrix, the characteristic polynomial can be obtained [12, 15, 18]. The polynomial is simplified by the fact that $k_{23} = k_{32} = 0$ in the mammillary model. Combining the polynomial with the Vieta formulas delivers the following basic relationships:

1.: $b_1 \times b_2 \times b_3 = k_{10} \times k_{21} \times k_{31}$

2.: $b_1 \times b_2 + b_1 \times b_3 + b_2 \times b_3 = k_{10} \times k_{31} + k_{21} \times k_{31} + k_{21} \times k_{13} + k_{10} \times k_{21} + k_{31} \times k_{12}$

3.: $b_1 + b_2 + b_3 = k_{10} + k_{12} + k_{13} + k_{21} + k_{31}$

Given the parameters from the compartment model in Figure 1 (k_{10}, k_{12}, etc.), the parameters describing the shape of the plasma concentration curve (b_1, c_1, etc.) can be computed as summarized in the following. This summary is based on the derivation given in the above cited references.

The following auxiliary quantities are defined:

$$a_0 = k_{10} \times k_{21} \times k_{31}$$

$$a_1 = k_{10} \times k_{31} + k_{21} \times k_{31} + k_{21} \times k_{13} + k_{10} \times k_{21} + k_{31} \times k_{12}$$

$$a_2 = k_{10} + k_{12} + k_{13} + k_{21} + k_{31}$$

$$p = a_1 - a_2^3 / 3$$

$$p = 2 \times a_2^3 / 27 - a_1 \times a_2 / 3 + a_0$$

$$r_1 = \sqrt{-(p^3/27)}$$

$$r_2 = 2 \times r_1^{1/3}$$

$$\varnothing = \arccos\left(-\frac{q}{2 \times r_1}\right) / 3$$

The solution for the plasma curve parameters is then:

$$b_1 = -(\cos(\varnothing) \times r_2 - a_2/3) \quad \{A1.2\}$$

$$b_2 = -\left(\cos(\varnothing + \frac{4 \times \pi}{3}) \times r_2 - a_2/3\right) \quad \{A1.3\}$$

$$b_3 = -\left(\cos(\varnothing + \frac{2 \times \pi}{3}) \times r_2 - a_2/3\right) \quad \{A1.4\}$$

$$c_1 = \frac{Q}{V_1} \times \frac{k_{21} - b_1}{b_1 - b_3} \times \frac{k_{31} - b_1}{b_1 - b_2} \quad \{A1.5\}$$

$$c_2 = \frac{Q}{V_1} \times \frac{k_{21} - b_2}{b_2 - b_3} \times \frac{k_{31} - b_2}{b_2 - b_1} \quad \{A1.6\}$$

$$c_3 = \frac{Q}{V_1} \times \frac{k_{21} - b_3}{b_3 - b_1} \times \frac{k_{31} - b_3}{b_3 - b_2} \quad \{A1.7\}$$

The concentrations in the other two compartments will follow sums of the same exponentials but with other factors.

For the peripheral fast compartment, the curve is:

$$C_{fast(t)} = F \times \exp(-b_1 \times t) + K \times \exp(-b_2 \times t) - (F+K) \times \exp(-b_3 \times t) \quad \{A1.8\}$$

where

$$F = \frac{Q}{V_1} \times \frac{k_{21} - b_1}{b_1 - b_3} \times \frac{k_{31}}{b_1 - b_2}, \quad \{A1.9\}$$

$$K = \frac{Q}{V_1} \times \frac{k_{21} - b_2}{b_2 - b_3} \times \frac{k_{31}}{b_2 - b_1}. \quad \{A1.10\}$$

For the peripheral slow compartment, the curve is:

$$C_{slow(t)} = H \times \exp(-b_1 \times t) + J \times \exp(-b_3 \times t) - (H+J) \times \exp(-b_2 \times t) \quad \{A1.11\}$$

where

$$H = \frac{Q}{V_1} \times \frac{k_{21}}{b_1 - b_3} \times \frac{k_{31} - b_1}{b_1 - b_2}, \quad \{A1.12\}$$

$$J = \frac{Q}{V_1} \times \frac{k_{21}}{b_3 - b_1} \times \frac{k_{31} - b_3}{b_3 - b_2}. \quad \{A1.13\}$$

Appendix 2. Calculation of the micro-constants from the hybrid-constants in the three-compartment mammillary model with central elimination

This appendix can be considered a reversal of the algorithm presented in Appendix 1. A similar algorithm is derived in [17].

Knowns: b_1, c_1, b_2, c_2, b_3, c_3; additionally, GFR_{fc} and ECV_{fc} can be calculated with the formulas given in the section II [Theory of the compartment model and GFR determination section].

At $t = 0$, activity Q is injected into V_1 (the plasma compartment), with no activity in V_2 and V_3. Total initial concentration is

$$C_1(0) = c_1 + c_2 + c_3,$$

leading to:

$$V_1 = \frac{Q}{c_3 + c_2 + c_3}. \quad \{A2.1\}$$

The excretion rate constant is

$$k_{10} = \frac{GFR_{fc}}{V_1}. \quad \{A2.2\}$$

For the mammillary model, $k_{23} = k_{32} = 0$. In the following, equations for k_{12}, k_{21}, k_{13} and k_{31} will be derived.

Calculation of the intercompartmental elimination rate constants:

The three-exponential plasma time-concentration formula {A1.1} is used. The derivative of $C_1(t)$ is the change of plasma (compartment 1) concentration for any time. Initial rate of change is:

$$dC_1/dt\,|_{t=0} = -c_1 \times b_1 - c_2 \times b_2 - c_3 \times b_3.$$

At $t = 0$ there is no tracer in compartments 2 and 3, so from the compartment model:

$$dC_1/dt\,|_{t=0} = -(k_{10} + k_{12} + k_{13}) \times C_1(0)$$

Equating these two expressions for the initial derivative and inserting $C_1(0)$, one receives:

$$k_{10} + k_{12} + k_{13} = \frac{c_1 \times b_1 + c_2 \times b_2 + c_3 \times b_3}{c_1 + c_2 + c_3}.$$

The variable P is defined as the sum of rate constants leading from the first compartment to the other compartments (but not excretion):

$$P = k_{12} + k_{13} = \frac{c_1 \times b_1 + c_2 \times b_2 + c_3 \times b_3}{c_1 + c_2 + c_3} - k_{10}\ .$$

where the rewriting allows calculation of P from the parameters known at this point.

The variable R is defined as the sum of rate constants leading into the first compartment:

$$R = k_{21} + k_{31} = b_1 + b_2 + b_3 - (k_{10} + k_{12} + k_{13})$$

where the latter equal sign follows from the third basic relationship (Appendix 1). Inserting the above equation for $k_{10} + k_{12} + k_{13}$ and rewriting, one receives:

$$R = k_{21} + k_{31} =$$

$$= \frac{c_2 \times b_1 + c_3 \times b_1 + c_1 \times b_2 + c_3 \times b_2 + c_1 \times b_3 + c_2 \times b_2}{c_1 + c_2 + c_3}$$

allowing calculation of R.

The variable S is defined as the product of k_{21} and k_{31}. From the first basic relationship (Appendix 1) one receives:

$$S = k_{21} \times k_{31} = b_1 \times b_2 \times b_3/k_{10}.$$

allowing calculation of S.

Combining the variables R and S, a quadratic equation in k_{21} can be set up and solved:

$$k_{21} = 0.5 \times \left(R - \sqrt{R^2 - 4 \times S}\right). \qquad \{A2.3\}$$

From the definition of R:

$$k_{31} = R - k_{21}. \qquad \{A2.4\}$$

The variable L is defined as a sum of products of the exponential constants (all of which are known, allowing calculation of L). From the second basic relationship:

$$L = k_{10} \times k_{31} + k_{21} \times k_{31} + k_{21} \times k_{13} + k_{10} \times k_{21} + k_{31} \times k_{12} =$$
$$= b_1 \times b_2 + b_1 \times b_3 + b_2 \times b_3,$$

The variable N is defined as:

$$N = k_{13} \times k_{21} + k_{12} \times k_{31} = L - R \times k_{10} - S.$$

Given the definition of P (and k_{21} and k_{31} already being calculated), this allows calculation of k_{12}:

$$k_{12} = \frac{N - P \times k_{21}}{(k_{31} - k_{21})}. \qquad \{A2.5\}$$

Finally, the last non-zero rate constant is

$$k_{13} = P - k_{12}. \qquad \{A2.6\}$$

Volumes of the peripheral compartments and intercompartmental clearances

From the relations mentioned in section II we get:

$$V_2 = V_1 \times k_{12}/k_{21} \qquad \{A2.7\}$$

$$V_3 = V_1 \times k_{13}/k_{31} \qquad \{A2.8\}$$

and

$$Cl_{12} = k_{12} \times V_1 \qquad \{A2.9\}$$

$$Cl_{13} = k_{13} \times V_1 \qquad \{A2.10\}$$

The mammillary model has $Cl_{23} = 0$.

Appendix 3. Calculation of the micro-constants from the hybrid-constants in the three-compartment catenary model with central elimination

Similarly as in the Appendix 1, the following basic relationships can be derived for the catenary model (where $k_{13} = k_{31} = 0$):

(1.): $b_1 \times b_2 \times b_3 = k_{10} \times k_{21} \times k_{31}$

(2.): $b_1 \times b_2 + b_2 \times b_3 + b_1 \times b_3 = k_{10} \times (k_{21} + k_{23} \times k_{32}) + k_{12} \times \times (k_{23} + k_{32}) + k_{21} \times k_{32}$

(3.): $b_1 + b_2 + b_3 = k_{10} + k_{12} + k_{23} + k_{32} + k_{21}$

Given are: b_1, b_2, b_3, c_1, c_2, c_3. Again, *GFR* and *ECV* can be calculated with equations {4} to {6}.

From these data, one may obtain:

$$C_1(0) = c_1 + c_2 + c_3$$

$$V_1 = Q/(c_1+c_2+c_3) \qquad \{A3.1\}$$

$$k_{10} = GFR/V_1 \qquad \{A3.2\}$$

As in Appendix 2:

$$dC_1/dt\ |_{t=0} = -c_1 \times b_1 - c_2 \times b_2 - c_3 \times b_3.$$

In the catenary model, there is no direct contact between the first and the third compartment, so the initial derivative from the model is different from Appendix 2:

$$dC_1/dt\ |_{t=0} = -(k_{10} + k_{12}) \times C_1(0)$$

Hence:

$$k_{12} = (c_1 \times b_1 + c_2 \times b_2 + c_3 \times b_3)/(c_1 + c_2 + c_3) - k_{10} \qquad \{A3.3\}$$

The variable R is defined as

$$R = k_{21} + k_{23} + k_{32} = b_1 + b_2 + b_3 - (k_{10} + k_{12})$$

where the third relation has been used.

The variable S is defined as:

$$S = k_{21} \times k_{32} = b_1 \times b_2 \times b_3/k_{10}$$

where the first relation has been used.

Using the second relation, the variable L is defined as:

$$L = k_{23} + k_{32}$$
$$= [b_1 \times b_2 + b_2 \times b_3 + b_1 \times b_3 - k_{21} \times k_{32} - k_{10} \times (k_{21} + k_{23} + k_{32})] / k_{12}$$
$$= [b_1 \times b_2 + b_2 \times b_3 + b_1 \times b_3 - S - k_{10} \times R] / k_{12}$$

R, S and L can all be computed from the input data and the already-computed k_{12}.

$$k_{21} = R - L \qquad \{A3.4\}$$

From the first relation:

$$k_{32} = b_1 \times b_2 \times b_3 / (k_{10} \times k_{21}) \quad \{A3.5\}$$

From the third relation:

$$k_{23} = b_1 + b_2 + b_3 - (k_{10} + k_{12} + k_{32} + k_{21}) \quad \{A3.6\}$$

Then:

$$V_2 = V_1 \times k_{12}/k_{21} \quad \{A3.7\}$$

$$V_3 = ECV - V_1 - V_2 \quad \{A3.8\}$$

$$Cl_{12} = k_{12} \times V_1 \quad \{A3.9\}$$

$$Cl_{23} = k_{23} \times V_2 \quad \{A3.10\}$$